SICE Annual Conference in Fukui, August 4-6, 2003
Fukui University, Japan

# MRAS Based Sensorless Control of Permanent Magnet Synchronous Motor

**Young Sam Kim, Sang Kyoon Kim and Young Ahn Kwon**

Department of Electrical Engineering , Pusan National University, Pusan 609-735, Korea
yakwon@pusan.ac.kr

**Abstract** - Speed and torque controls of permanent magnet synchronous motors are usually attained by the application of position and speed sensors. However, speed and position sensors require the additional mounting space, reduce the reliability in harsh environments and increase the cost of a motor. Therefore, many studies have been performed for the elimination of speed and position sensors. This paper investigates a novel speed sensorless control of a permanent magnet synchronous motor. The proposed control strategy is based on the MRAS(Model Reference Adaptive System) using the state observer model with the current error feedback and the magnet flux model as two models for the back-EMF estimation. The proposed algorithm is verified through the simulation and experiment.

**Keywords** : Permanent Magnet Synchronous Motor, Sensorless Control, Model Reference Adaptive System.

## Ⅰ. Introduction

The vector control in the speed and torque controlled ac drive is widely used for a high performance application. The vector control of a permanent magnet synchronous motor is usually implemented through measuring the speed and position. However, speed and position sensors require the additional mounting space, reduce the reliability in harsh environments and increase the cost of a motor. Various control algorithms have been proposed for the elimination of speed and position sensors: estimators using state equations, Luenberger or Kalman-filter observers, sliding mode control, saliency effects, artificial intelligence, direct control of torque and flux, and so on[1-4]. This paper proposes the control strategy based on the MRAS(Model Reference Adaptive System) in the sensorless control of a permanent magnet synchronous motor. The MRAS algorithm is well-known in the sensorless control of an induction motor, and has been proved to be effective and physically clear[5-7]. The MRAS algorithm is based on the comparison between the outputs of two estimators. The error between the estimated quantities obtained by the two models is used to drive a suitable adaptation mechanism which generates the estimated rotor speed. The MRAS proposed in this paper is using the state observer model with the current error feedback and the magnet flux model as two models for the back-EMF estimation. The proposed algorithm is verified through the simulation and experiment.

## Ⅱ. Mathematical Modeling of PMSM

Fig. 1 shows the equivalent model of a permanent magnet synchronous motor. $R_a$ and $L_a$ in Fig. 1 indicate the equivalent resistance and inductance. Flux reference axes are also shown in Fig. 1.

The stator voltage equations in the real axes may be expressed as

$$\begin{aligned} v_{as} &= R_a i_{as} + \frac{d\psi_{as}}{dt} \\ &= R_a i_{as} + \frac{3}{2} L_a \frac{di_{as}}{dt} + e_{as} \end{aligned} \tag{1}$$


PR0001/03/0000-0132 ¥400 © 2003 SICE

Elearnica
Downloaded from http://www.elearnica.ir

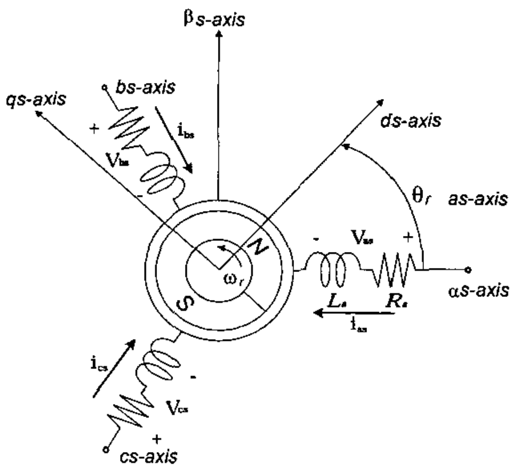


Fig. 1 The Equivalent model of 3-phase PMSM

$$v_{bs} = R_a i_{bs} + \frac{d\psi_{bs}}{dt} = R_a i_{bs} + \frac{3}{2} L_a \frac{di_{bs}}{dt} + e_{bs} \quad (2)$$

$$v_{cs} = R_a i_{cs} + \frac{d\psi_{cs}}{dt} = R_a i_{cs} + \frac{3}{2} L_a \frac{di_{cs}}{dt} + e_{cs} \quad (3)$$

where the back-EMFs of the phase windings induced from the flux of the permanent magnet are as follows.

$$e_{as} = \frac{d\psi_{af}}{dt} = -\omega_r K_E \sin\theta_r \quad (4)$$

$$e_{bs} = \frac{d\psi_{bf}}{dt} = -\omega_r K_E \sin(\theta_r - \frac{2}{3}\pi) \quad (5)$$

$$e_{bs} = \frac{d\psi_{cf}}{dt} = -\omega_r K_E \sin(\theta_r - \frac{4}{3}\pi) \quad (6)$$

where $\omega_r = \frac{d\theta_r}{dt}$ and $K_E$ is the back-EMF constant.

From (1) - (3), $\alpha$ - and $\beta$ - axis voltage equations in the stationary reference frame fixed to the stator may be expressed as

$$v_{\alpha s} = R_s i_{\alpha s} + L_s \frac{di_{\alpha s}}{dt} + e_{\alpha s} \quad (7)$$

$$v_{\beta s} = R_s i_{\beta s} + L_s \frac{di_{\beta s}}{dt} + e_{\beta s} \quad (8)$$

where $R_s = R_a$ and $L_s = \frac{3}{2} L_a$.

$$e_{\alpha s} = \frac{d\psi_{\alpha f}}{dt} = -\omega_r K_e \sin\theta_r \quad (9)$$

$$e_{\beta s} = \frac{d\psi_{\beta f}}{dt} = \omega_r K_e \cos\theta_r \quad (10)$$

where $K_e = \sqrt{\frac{3}{2}} K_E$.

From (1) - (3), $d$ - and $q$ - axis voltage equations in the rotor reference frame with the rotating speed of $\omega_r$ may be expressed as

$$v_{ds} = R_s i_{ds} + L_s \frac{di_{ds}}{dt} - \omega_r L_s i_{qs} \quad (11)$$

$$v_{qs} = R_s i_{qs} + L_s \frac{di_{qs}}{dt} + \omega_r L_s i_{ds} + \omega_r K_e \quad (12)$$

The electromagnetic torque in the rotor reference frame may be expressed as

$$T = P K_e i_{qs} \quad (13)$$

where $P$ is the number of poles.

The mechanical equation of a PMSM may be expressed as

$$T = J \frac{d\omega_m}{dt} + D\omega_m + T_L \quad (14)$$

where $J$ is the inertia coefficient and $D$ is the friction coefficient, $\omega_m$ is the mechanical speed of the rotor, and $T_L$ is the load torque.

# Ⅲ. MRAS Based Sensorless Control

This paper proposes a novel sensorless control algorithm based on the MRAS. In general the MRAS algorithm is based on the comparison between the outputs of two estimators. The error between the estimated quantities obtained by the two models is used to drive a suitable adaptation mechanism which generates the estimated rotor speed. The MRAS algorithm is well-known in the sensorless control of an induction motor, and has been proved to be effective and physically clear[5-7]. The MRAS proposed in this paper is using the state observer model with the current error feedback and the magnet flux model as two models for the back-EMF estimation.

## A. State observer configuration

From (7) and (8), the state equations of the full order observer in the stationary reference frame may be expressed as

$$\dot{\hat{\mathbf{x}}} = \mathbf{A}\hat{\mathbf{x}} + \mathbf{B}\,\mathbf{v}_s + \mathbf{L}(\mathbf{i}_s - \hat{\mathbf{i}}_s) \tag{15}$$

$$\hat{\mathbf{i}}_s = \mathbf{C}\,\hat{\mathbf{x}} \tag{16}$$

where ^ means the estimated value, $\mathbf{L}$ is the observer gain and $\mathbf{x}=\begin{bmatrix}\mathbf{i}_s\\ \mathbf{e}_s\end{bmatrix}$, $\mathbf{i}_s=\begin{bmatrix}i_{\alpha s}\\ i_{\beta s}\end{bmatrix}$, $\mathbf{e}_s=\begin{bmatrix}e_{\alpha s}\\ e_{\beta s}\end{bmatrix}$, $\mathbf{v}_s=\begin{bmatrix}v_{\alpha s}\\ v_{\beta s}\end{bmatrix}$,

$$\mathbf{A}=\begin{bmatrix}\mathbf{A}_{11}\,\mathbf{A}_{12}\\ \mathbf{A}_{21}\,\mathbf{A}_{22}\end{bmatrix},\ \mathbf{A}_{11}=\begin{bmatrix}-R_s/L_s & 0\\ 0 & -R_s/L_s\end{bmatrix},$$

$$\mathbf{A}_{12}=\begin{bmatrix}-1/L_s & 0\\ 0 & -1/L_s\end{bmatrix},\ \mathbf{A}_{21}=\begin{bmatrix}0 & 0\\ 0 & 0\end{bmatrix},\ \mathbf{A}_{22}=\begin{bmatrix}0 & -\omega_r\\ \omega_r & 0\end{bmatrix},$$

$$\mathbf{B}=\begin{bmatrix}\mathbf{B}_1\\ \mathbf{B}_2\end{bmatrix},\ \mathbf{B}_1=\begin{bmatrix}1/L_s & 0\\ 0 & 1/L_s\end{bmatrix},\ \mathbf{B}_2=\begin{bmatrix}0 & 0\\ 0 & 0\end{bmatrix},$$

$$\mathbf{C}=\begin{bmatrix}1 & 0 & 0 & 0\\ 0 & 1 & 0 & 0\end{bmatrix}.$$

Here, the estimated currents may be replaced by the measured currents, and the order of the observed states may be reduced. This paper uses the reduced order observer which may be expressed as follows:

$$\dot{\hat{\mathbf{w}}} = \mathbf{F}\hat{\mathbf{w}} + \mathbf{D}\mathbf{i}_s + \mathbf{G}\mathbf{v}_s \tag{17}$$

$$\hat{\mathbf{z}} = \hat{\mathbf{w}} + \mathbf{L}\mathbf{i}_s \tag{18}$$

where $\hat{\mathbf{z}} = \left[\hat{e}_{\alpha s}\ \ \hat{e}_{\beta s}\right]^T$, $\hat{\mathbf{w}} = \left[\hat{w}_1\ \ \hat{w}_2\right]^T$,

$$\mathbf{F} \equiv \mathbf{A}_{22} - \mathbf{L}\mathbf{A}_{12},$$
$$\mathbf{D} \equiv \mathbf{F}\mathbf{L} + \mathbf{A}_{21} - \mathbf{L}\mathbf{A}_{11},$$
$$\mathbf{G} \equiv \mathbf{B}_2 - \mathbf{L}\mathbf{B}_1.$$

Fig. 2 shows the block diagram of the reduced order state observer for the back-EMF estimation.

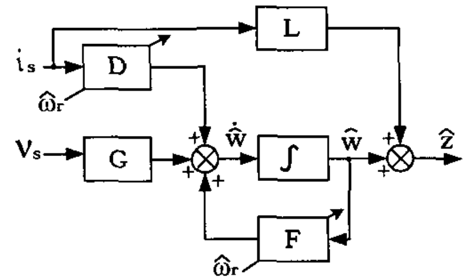


Fig. 2 Block diagram of the reduced order state observer

## B. MRAS configuration

This paper proposes a novel sensorless control algorithm based on the MRAS for the speed sensorless control of a PMSM. The proposed MRAS is using the state observer model of (17) and (18) and the magnet flux model of (9) and (10) as two models for the back-EMF estimation. The rotor speed is generated from the adaptation mechanism using the error between the estimated quantities obtained by the two models as follows:

$$\hat{\omega}_r = K_p(\hat{e}_{\beta s}\tilde{e}_{\alpha s} - \hat{e}_{\alpha s}\tilde{e}_{\beta s}) + K_i\int(\hat{e}_{\beta s}\tilde{e}_{\alpha s} - \hat{e}_{\alpha s}\tilde{e}_{\beta s})\,dt \tag{19}$$

where $K_p$ and $K_i$ are the gain constants, $\hat{e}_{\alpha s}$ and $\hat{e}_{\beta s}$ are the estimated values of back-EMFs in the state observer model, and $\tilde{e}_{\alpha s}$ and $\tilde{e}_{\beta s}$ are the estimated values of back-EMFs in the magnet flux model.

Fig. 3 shows the block diagram of the proposed MRAS. The proposed MRAS algorithm has a robust performance through combining the state observer model and the magnet flux model.

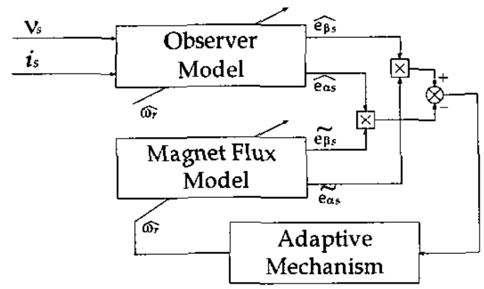


Fig. 3 Block diagram of the proposed MRAS

The overall system of the proposed sensorless control algorithm is shown in Fig. 4.

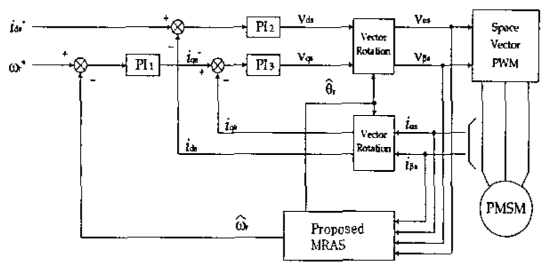


Fig. 4 Configuration of the overall system

## Ⅳ. Simulation

The simulation has been performed for the verification of the proposed control algorithm. Table 1 shows the specification of the permanent magnet synchronous motor used in the simulation and experiment.

Table 1 Motor specification

| | | | |
|---|---|---|---|
| Number of pole | 8 | Rs | 1.0 Ω |
| Nominal current | 5.3 A | Ls | 4.17 mH |
| Nominal power | 750 W | Ke | 0.132 Vsec/rad |

Fig. 5 (a), (b) and (c) show the speed responses in the speed commands of 50rpm, 200rpm and 1000rpm and in the no load. As shown in Fig. 5, the proposed sensorless control algorithm has good speed responses in the low and high speeds.

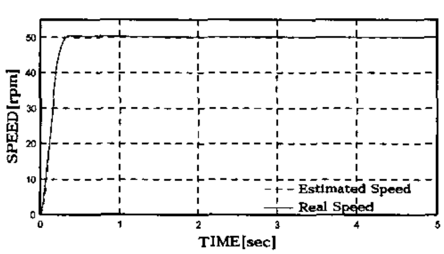


(a)

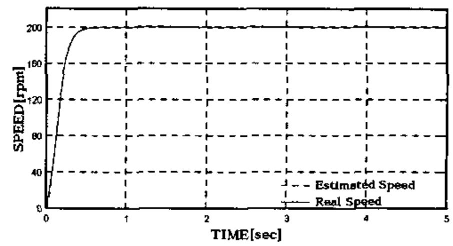


(b)

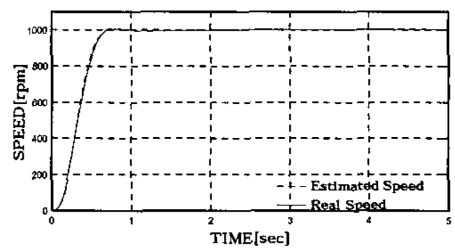


(c)

Fig. 5 Speed responses in the speed command of (a) 50 rpm (b) 200 rpm (c) 1000 rpm

Fig. 6 and Fig. 7 show the speed responses in case of considering the parameter variations where the stator winding resistance is increased by 50% of the nominal value and the back EMF constant is decreased by 20% of the nominal value. The parameter variations are applied in the middle of the operation of 200rpm and no-load. For the comparison with the conventional state observer sensorless control algorithm, the simulation is also performed under the same conditions. The simulation result shows an improved and robust performance in the proposed sensorless control algorithm.

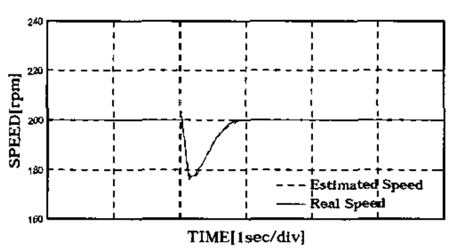


(a)

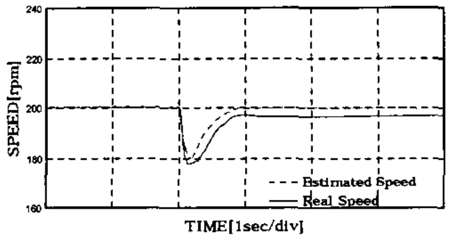


(b)

Fig. 6 Speed responses in a stator resistance variation

( $\hat{R}_s = 1.5R_s$ , 200 rpm )

(a) Proposed MRAS (b) State observer

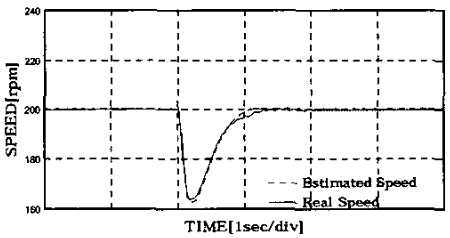


(a)

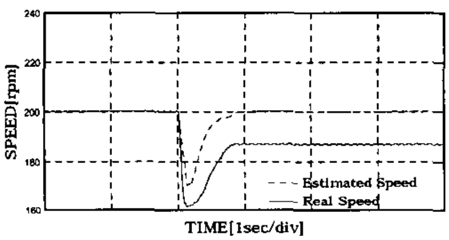


(b)

Fig. 7 Speed responses in a back-EMF constant

variation ( $\hat{K}_e = 0.8K_e$ , 200 rpm )

(a) Proposed MRAS (b) State observer

# V. Experiments and Discussions

The experiments have been performed for the verification of the proposed control algorithm. The microprocessor system(80586/150MHz) is used for the digital processing of the proposed algorithm.

Fig. 8 (a), (b) and (c) show the experimental speed responses in the speed commands of 50rpm, 200rpm and 1000rpm and in the no load. The proposed sensorless control algorithm has good speed responses in the low and high speeds same as the simulation result.

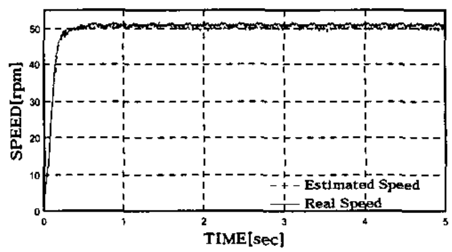


(a)

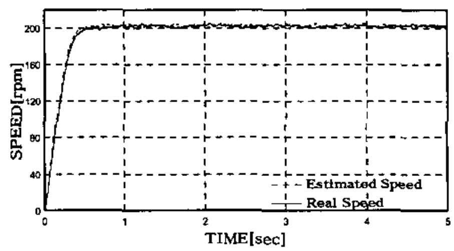


(b)

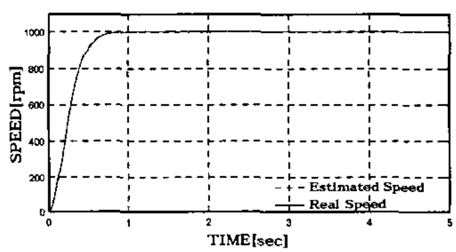


(c)

Fig. 8 Experimental speed responses in the speed command of (a) 50 rpm (b) 200 rpm (c) 1000 rpm

Fig. 9 and Fig. 10 show the experimental speed responses in case of considering the parameter variations where the stator winding resistance is increased by 50% of the nominal value and the back EMF constant is decreased by 20% of the nominal value. The parameter variations are applied in the middle of the operation of 200rpm and no-load. For the comparison with the conventional state observer sensorless control algorithm, the experiment is also performed under the same conditions. The experimental result shows an improved and robust performance in the proposed sensorless control algorithm.

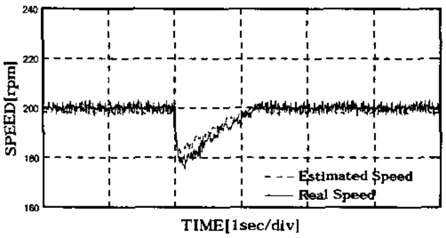


(a)

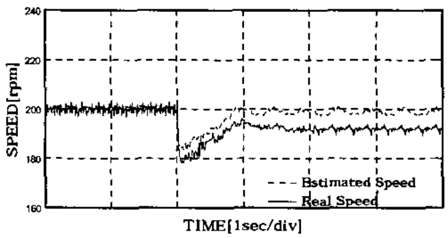


(b)

Fig. 9 Experimental speed responses in a stator resistance variation ( $\hat{R}_s = 1.5R_s$ , 200 rpm )

(a) Proposed MRAS (b) State observer

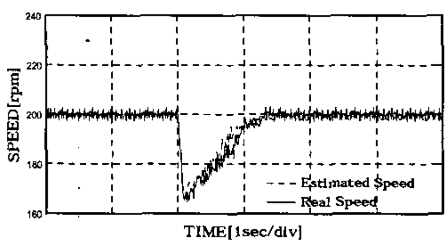


(a)

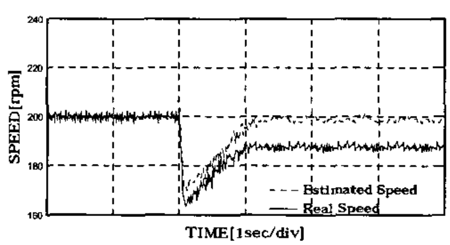


(b)

Fig. 10 Experimental speed responses in a back-EMF constant variation ( $\hat{K}_e = 0.8K_e$ , 200 rpm )

(a) Proposed MRAS (b) State observer

# Ⅵ. Conclusions

This paper proposed a novel speed sensorless control algorithm of a permanent magnet synchronous motor. The proposed control algorithm is based on the MRAS using the state observer model and the magnet flux model as two models for the back-EMF estimation. The rotor speed is generated from the adaptation mechanism using the error between the estimated quantities obtained by the two models.

The simulation and experimental results indicate that the proposed algorithm shows good speed responses in the low and high speeds, and shows robust speed responses in the stator resistance and back-EMF variations. Especially, the proposed algorithm shows a better performance in the parameter variation compared to the conventional algorithm.

# Ⅶ. References


[1] Edited by K. Rajashekara, A. Kawamura and K. Matsuse, *Sensorless Control of AC Motor Drives,* IEEE Press, 1996.

[2] J. Holtz, "State of the Art of Controlled AC Drives without Speed Sensors," Int. J. Electronics, Vol. 80, No. 2, pp. 249-263, 1996.

[3] C. Ilas, A. Bettini, L. Ferraris, and F. Profumo, "Comparison of Different Schemes without Shaft Sensors for Field Oriented Control Drives," IEEE Proc. IECON, pp. 1579-1588, 1994.

[4] P. Vas, *Sensorless Vector and Direct Torque Control,* Oxford Univ. Press, 1998.

[5] C. Schauder, "Adaptive Speed Identification for Vector Control of Induction Motors without Rotational Transducers," IEEE Trans Ind Appl, Vol. 28, No. 5, pp. 1054-1061, 1992.

[6] F. Z. Peng and T. Fukao, "Robust Speed Identification for Speed-Sensorless Vector Control of Induction Motors," IEEE Trans Ind Appl, Vol. 30, No.5, pp. 1234-1240, 1994.

[7] Y. A. Kwon and D. W. Jin, "A Novel MRAS Based Speed Sensorless Control of Induction Motor," IEEE Proc IECON, Vol. , pp. 933-938, 1999.